Textile Science & Research Journal
ISSN: 3059-846X, Volume – 2, Issue – 1, 2026
DOI: https://doi.org/10.63456/tsrj-2-1-39

MODELING THE VISCOELASTIC BEHAVIOR OF SEWN MULTI-LAYER INSULATION FABRICS: A NON-LINEAR RESPONSE AND OPTIMAL NUMBER OF LAYERS

ZAHRA JAMSHIDI [1,*], SAEED AJELI [2], MEHDI SALMANI-TEHRANI [3]

[1] Department of Textile Engineering, Isfahan University of Technology, Isfahan, 84156-83111, Iran. z.jamshidi1991@gmail.com

[2] Department of Textile Engineering, Isfahan University of Technology, Isfahan, 84156-83111, Iran. sajeli@iut.ac.ir

[3] Department of Mechanical Engineering, Isfahan University of Technology, Isfahan, 84156-83111, Iran. Tehrani@iut.ac.ir

Zahra Jamshidi : z.jamshidi1991@gmail.com

Corresponding author: ZAHRA JAMSHIDI

ABSTRACT

Investigating the time-dependent mechanical behavior of hybrid multi-layer textile structures, designed for high-performance technical applications, is critical for ensuring their dimensional stability. This study comprehensively investigates the influence of the number of layers (2, 6, 12, and 24) on the viscoelastic creep mechanism within the seam zone of these structures. To this end, a dual-analysis methodology was employed, incorporating mathematical modeling using the four-parameter Burgers model (based on independent parameters E_M, η_M, E_V, and η_V) and a complementary phenomenological analysis based on creep rate, applied to both seamed and seamless specimens. The results revealed a non-linear relationship between the number of layers and the viscoelastic properties. Mechanical performance peaked in the 12-layers structure, where the instantaneous elastic modulus (E_M) reached a maximum of 459.10 ± 9.33 MPa. Comparative analysis demonstrated that the seam plays a dual role: acting as a stiffness-weakening factor in thin structures (2 layers), while functioning as a mechanism that significantly enhances structural resistance against permanent deformation in thick structures (24 layers). The most significant finding was the critical role of the seam in the 12-layers structure; here, the stitched seam transformed an inherently unstable structure into an optimal structure with superior structural cohesion, acting as a stabilizing and reinforcing agent. These findings highlight the necessity of understanding the complex interaction between the seam and the multi-layer assembly for the optimal design of structures requiring high dimensional stability.

KEYWORDS: Multi-layer textile structures, Viscoelastic creep behavior, Burgers model, Seam mechanics

1. INTRODUCTION

Multi-Layer hybrid textile structures, composed of textile sheets and high reflective radiation shields, have emerged as one of the most efficient solutions for achieving high strength-to-weight ratios in high-performance technical applications [1]. These structures have garnered particular attention in the fabrication of flexible thermal insulation systems, as multiple layers of reflective films can effectively attenuate radiative heat transfer, while spacer fabrics—in addition to enhancing structural strength—prevent interlayer contact and mitigate thermal bridging [2-5]. To fabricate these flexible structures into functional configurations, joining the constituent layers via seam formation is inevitable. During the sewing process, the seam zone—serving as the interface between textile components and polymeric films—is frequently subjected to various mechanical stresses, including presser foot pressure, sewing thread tension, and localized compression induced by thread retraction within the fabric structure [6, 7]. Consequently, the seam functions as a potential locus of weakness, compromising the mechanical performance of the entire structure [8-10]. Furthermore, under operational conditions, these structures are often subjected to static mechanical loads, such as installation-induced stresses and thermal stresses resulting from temperature fluctuations [11]. Given that the primary constituents of these structures—namely polymeric films, sewing threads, and fabrics—possess an inherent viscoelastic nature, they undergo time-dependent deformation, or Creep, when subjected to constant loading [12-14].This creep phenomenon can precipitate permanent deformation, strength degradation, dimensional instability, and even delayed failure [15]. Therefore, creep analysis and precise modeling are prerequisites for the design of soft structures intended for critical applications, as the time-dependent behavior of these materials directly impacts their dimensional stability and long-term performance.

From a mechanical perspective, all components of the compound material in question, including the fabric, polymeric film and the seam zone, are anisotropic and exhibit non-linear behavior with respect to stress, time, and temperature. Consequently, the viscoelastic behavior of the seam zone is expected to be a function not only of intrinsic material properties but also of structural factors such as local thickness, the number of layers, and the degree of relative slippage and friction between layers. Such complexity underscores the necessity of employing more precise analytical approaches.

Previous studies on the mechanical behavior of multilayered seams have predominantly focused on ultimate tensile strength under short—term loading regimes, with limited attention directed toward time-dependent behavior [16-20].

Textile Science & Research Journal
ISSN: 3059-846X, Volume – 2, Issue – 1, 2026
DOI: https://doi.org/10.63456/tsrj-2-1-39

Furthermore, mathematical viscoelastic models, such as the Burgers model, have been widely employed to characterize the creep behavior of polymers and textiles, demonstrating significant capability in decoupling instantaneous, delayed, and viscous flow deformation mechanisms [21, 22]. However, the influence of structural parameters—specifically the number of layers—on the viscoelastic behavior and seam creep in multi-layer structures has not yet been comprehensively investigated.

To ensure the dimensional stability of technical insulation fabrics, the optimal performance is defined as a synergistic balance between high mechanical stiffness (maximum E_M and E_V) and maximum viscous resistance against both delayed and permanent deformation (maximized independent parameters η_V , η_M). This combination of fundamental viscoelastic parameters serves as the criterion for identifying the most efficient structural configuration among the investigated multi-layer assemblies.

Accordingly, the present study addresses this gap by conducting a comprehensive investigation into the creep behavior of the seam zone in thermal insulation structures with varying numbers of layers (2, 6, 12, and 24). To achieve this objective, a dual-analysis methodology was employed, incorporating mathematical modeling using the four-parameter Burgers model—based on the independent parameters E_M, η_M, E_V, and η_V—and a complementary phenomenological analysis based on creep rate. This approach was applied to both seamed and seamless (control) specimens to provide a deep and multifaceted understanding of the complex interaction between the seam structure and the number of layers.

2. MATERIALS AND METHODS

In this study, double- side aluminized Mylar polyester films with a thickness of 0.5 µm were employed. Additionally, perforated warp-knitted net fabrics was utilized as spacers to separate the polymeric films, and 100% polyester sewing threads were used to stitch and join the layers. The specifications of the polymeric film, fabric, and sewing thread used in this research are presented in Table 1.

Table 1. Technical characteristics of hybrid multi-Layer textile structures components.

Component	Material Type	Thickness (µm)	Yarn Count (tex)	Areal Density ($g.m^{-2}$)	CPC/WPC (cm^{-1})	Tenacity (cN/tex)	Elongation (%)
Knitted Fabric	100% Polyester Warp Knitted Voile	181	4.87	36.94	12/12	-	-
Sewing Thread	100% Polyester	-	72	-	-	38.67	16.36
Polymer Film	BoPET Polyester Film (metalized by 0.5 µm Aluminum)	12	-	-	-	-	-

To fabricate the multi-layer structures, the polymeric film layers and knitted net fabrics were stacked in an alternating sequence. The sewing operation was executed using an industrial sewing machine (Jack, Model JK-9100B, China) at a speed of 4000 stitches per minute. Regarding the seam configuration, a lapped superimposed seam (Class LSa-1) was selected to define the layer arrangement at the seam region, employing a standard lock stitch (Class 301). To minimize thermal leakage at the seam area, a layer overlap of 1.0 inch and a seam allowance of 0.5 inches from the fabric edge were adopted, in accordance with standard recommendations [23]. Fig. 1 illustrates the schematic representation of the alternating arrangement of layers, the utilized seam and stitch type, as well as the layer overlap and seam allowance dimensions.

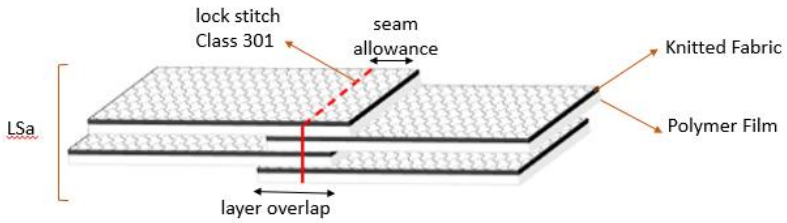

Figure 1. Schematic representation of the seam assembly, layer arrangement, and geometrical dimensions.

Prior to the main experimental phase, a series of preliminary experiments were conducted to optimize the sewing parameters, aiming to achieve a stable and structurally integrated assembly. Accordingly, all specimens in this study were sewn using the optimized parameters, comprising a needle foot pressure of 16.28 N , a needle thread tension of 13.52 N, and a stitch density of 5 SPI.

2.1. TENSILE TESTING

To characterize the fundamental mechanical properties, specifically the Ultimate Tensile Strength (UTS), tensile tests were conducted on both seamed and seamless specimens in accordance with ASTM D1683-04. The experiments were executed

using a Zwick universal testing machine operating at a Constant Rate of Extension (CRE). A gauge length of 75 mm and a crosshead speed of 300 mm/min were employed. The load was applied perpendicular to the seam line and aligned with the wale direction of the warp-knitted spacer fabric. For each sample configuration, five replicates were tested, and the mean values along with the standard deviations were reported. The dimensions of the seamed specimens were 175 × 100 mm, while the seamless specimens measured 200 ×100 mm.

2.2. CREEP TEST

The viscoelastic behavior of the samples under constant loading conditions was evaluated using creep testing. The tests were conducted on multi-layer specimens with varying numbers of layers (2, 6, 12, and 24), fabricated using the optimized sewing parameters described earlier. Each specimen was subjected to a constant tensile load equivalent to 60% of its specific Ultimate Tensile Strength (UTS). Since the UTS significantly varied with the number of layers, the magnitude of the applied static load was adjusted for each specimen type (2, 6, 12, and 24 layers) to maintain a consistent stress level relative to its strength. The experiments were carried out under controlled environmental conditions at a temperature of 20 ℃. In the experimental setup, the upper clamp was fixed, while a constant static load was applied to the lower clamp. To eliminate potential errors caused by specimen slippage within the clamps, two distinct horizontal markers were placed directly on the specimen surface. The initial distance between these markers was defined as the reference gauge length. The upper marker, positioned near the fixed clamp, served as the stationary coordinate reference point. The specimen elongation was recorded using a non-contact image processing technique at 1-minute intervals for the first 10 minutes, followed by 10-minute intervals up to the total duration of 120 minutes. The instantaneous elongation recorded at the onset of loading (t=0) was utilized to calculate the instantaneous elastic strain, providing the physical basis for determining the Maxwell elastic modulus in the subsequent modeling stage. To ensure the reproducibility of the results, four replicates were tested for each sample configuration. Fig. 2 illustrates the seamed specimen undergoing creep testing.

Figure 2. Experimental setup of the seamed specimen undergoing creep testing.

2.3. DATA ANALYSIS METHODOLOGY

To enhance the reliability of the results and establish a comprehensive analytical framework, a dual-analysis methodology was employed in this study. This strategy facilitates the cross validation of findings and comprises two main components:

1. Parametric Analysis: Utilizing viscoelastic mathematical modeling to extract and quantify the physical parameters governing the material behavior.
2. Phenomenological Analysis: A model-independent approach based on creep rate assessment to provide direct observation and visual verification of the deformation process dynamics.

The final results and conclusions of this research are grounded in the convergence of findings derived from these two independent methods.

2.4. VISCOELASTIC MODELING

The time-dependent deformation behavior of multi-layer textile structures under constant loading originates from the inherent viscoelastic nature of the constituent polymers and their geometrical structure. To quantitatively describe this

Textile Science & Research Journal
ISSN: 3059-846X, Volume – 2, Issue – 1, 2026
DOI: https://doi.org/10.63456/tsrj-2-1-39

behavior, a rheological modeling approach was employed, wherein the mechanical response of the material is simulated using a combination of ideal spring and dashpot elements.

Ideal Spring: Represents linear elastic behavior (Hooke's Law), where stress (σ) is proportional to strain (ε):

$$\sigma = E\,.\,\varepsilon \qquad (1)$$

where E is the elastic modulus.

Ideal Dashpot: Represents Newtonian viscous behavior, where stress is proportional to the strain rate ($d\varepsilon/dt$):

$$\sigma = \eta\,.\frac{d\varepsilon}{dt} \qquad (2)$$

where η is the viscosity coefficient.

To select the optimal model, various candidate models, including the Power Law model and hybrid models, were initially evaluated. These models were discarded due to non-convergence in fitting experimental data and the generation of parameters lacking physical meaning (e.g., negative values). Ultimately, the four-parameter Burgers model, schematically illustrated in Fig. 3, was selected as the governing model. This model, composed of a Maxwell unit connected in series with a Kelvin-Voigt unit, possesses a unique capability to decouple and quantify three primary deformation mechanisms.

The total strain in the Burgers model is the sum of the strains in the Maxwell and Kelvin-Voigt units. Consequently, the constitutive equation governing the mechanical behavior of this model can be expressed in its differential form as follows:

$$\sigma + \left(\frac{\eta_M}{E_M} + \frac{\eta_M}{E_V} + \frac{\eta_V}{E_V}\right)\dot{\sigma} + \frac{\eta_M\,\eta_V}{E_M\,E_V}\,\ddot{\sigma} = \eta_M\,\dot{\varepsilon} + \frac{\eta_M\,\eta_V}{E_V}\,\ddot{\varepsilon} \qquad (3)$$

Solving this differential equation for a creep test condition (where stress $\sigma = \sigma_0$ is constant, thus $\dot{\sigma} = 0$ and $\ddot{\sigma} = 0$) yields the time-dependent strain formulation presented in Eq. (4).

By applying a constant stress (σ_0) in the creep test (t > 0), the time-dependent creep strain response for the Burgers model is obtained by solving the constitutive equation (Eq. 3) as follows:

$$\varepsilon(t) = \frac{\sigma_0}{E_M} + \frac{\sigma_0}{E_V}\left(1 - e^{-\frac{E_V\,.t}{\eta_V}}\right) + \frac{\sigma_0}{\eta_M}t \qquad (4)$$

Where:

$\frac{\sigma_0}{E_M}$: Instantaneous elastic strain (Maxwell spring component).

$\frac{\sigma_0}{E_v}\left(1 - e^{-\frac{E_V\,.t}{\eta_V}}\right)$: Delayed viscoelastic strain (Kelvin-Voigt component).

$\frac{\sigma_0\,.t}{\eta_M}$: Permanent viscous flow (Maxwell dashpot component).

The schematic creep response curve corresponding to this constitutive equation is illustrated in Fig. 4, which visually distinguishes these three deformation regions (instantaneous, delayed, and viscous)

Textile Science & Research Journal
ISSN: 3059-846X, Volume – 2, Issue – 1, 2026
DOI: https://doi.org/10.63456/tsrj-2-1-39

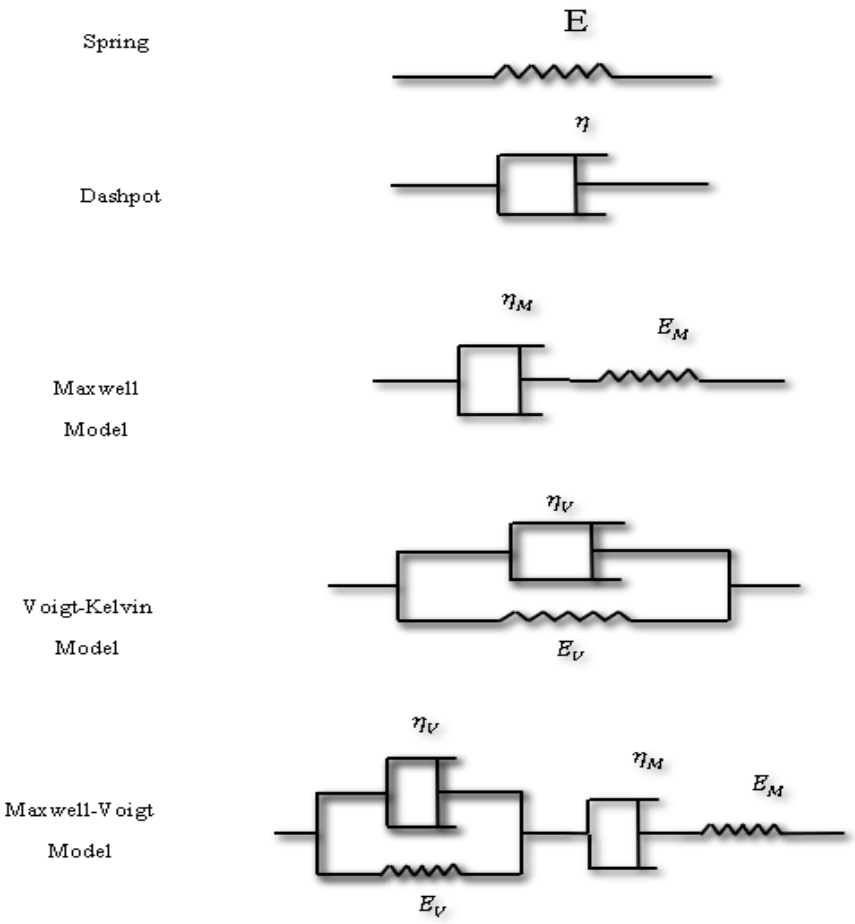

Figure 3. Schematic representation of the viscoelastic modeling approach: basic spring and dashpot mechanical elements, the four-parameter Burgers model structure composed of Maxwell and Kelvin-Voigt units in series.

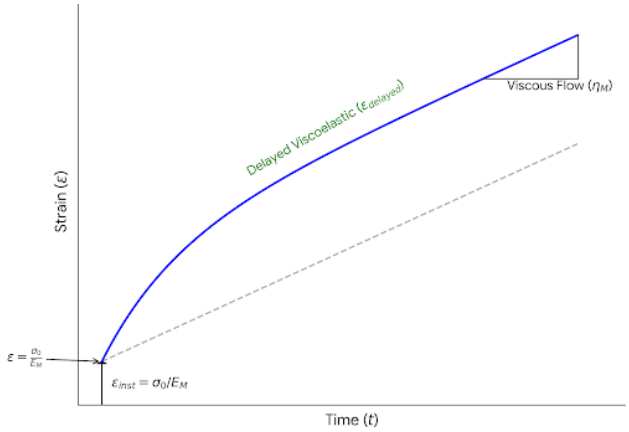

Figure 4. Theoretical creep strain response under constant stress, comprising instantaneous elastic, delayed viscoelastic, and permanent viscous flow components.

The four independent material parameters of the model (E_M, η_M, E_V, and η_V) were fitted to the experimental data using the Non-linear Least Squares Regression method. It should be noted that the applied stress (σ_0) was treated as a known experimental constant specific to each layer configuration—calculated based on the 60% UTS loading level— rather than a fitted variable, to ensure the physical consistency of the estimated material constants. The Gauss-Newton iterative algorithm was utilized to minimize the Sum of Squared Errors (SSE) between the experimental data and the model predictions. The goodness-of-fit was evaluated using the coefficient of determination (R^2) and the Root Mean Square Error (RMSE). To maintain statistical rigor, the final material constants are reported as the mean value ± standard deviation of four replicates for each sample type. The high concordance between the model curves and the experimental data —supported by R^2 values

Textile Science & Research Journal
ISSN: 3059-846X, Volume – 2, Issue – 1, 2026
DOI: https://doi.org/10.63456/tsrj-2-1-39

consistently exceeding 0.98— confirms the efficacy of this model in characterizing the complex creep behavior of the multi-layer structures.

2.5. CREEP RATE ANALYSIS

As a complementary approach independent of parametric modeling, the creep rate (dε/dt) was calculated using the central difference numerical differentiation method, according to Eq. (5):

$$\text{Creep Rate}(t_i) = \frac{\varepsilon_{i+1} - \varepsilon_{i-1}}{t_{i+1} - t_{i-1}} \quad (5)$$

The primary objective of this analysis was to provide visual and physical verification of the dynamics extracted from the modeling parameters—specifically the retardation time (τ) —and to gain a deeper insight into the transition stages of the material's behavior. To this end, the results were plotted on a log-log scale to facilitate a clearer distinction between the primary creep and secondary creep stages.

3. RESULTS AND DISCUSSION

3.1. MODEL VALIDATION

The quantitative evaluation of the experimental data confirmed the high efficacy of the four-parameter Burgers model in characterizing the viscoelastic behavior of the studied structures. As illustrated in Fig. 5, the model predictions exhibited excellent agreement with the experimental creep curves. Furthermore, the high values of the coefficient of determination ($R^2 > 0.98$) and low Root Mean Square Error (RMSE) across the fitted datasets provide robust statistical evidence for the model's validity. Consequently, this model effectively decoupled the independent deformation parameters—including E_M, E_V, η_V and η_M— thereby justifying its deployment for further parametric analysis. It is noteworthy that the 12-layer seamless specimen constituted the sole exception where mathematical convergence was not achieved due to extreme structural instability; this specific anomaly is addressed in the subsequent section.

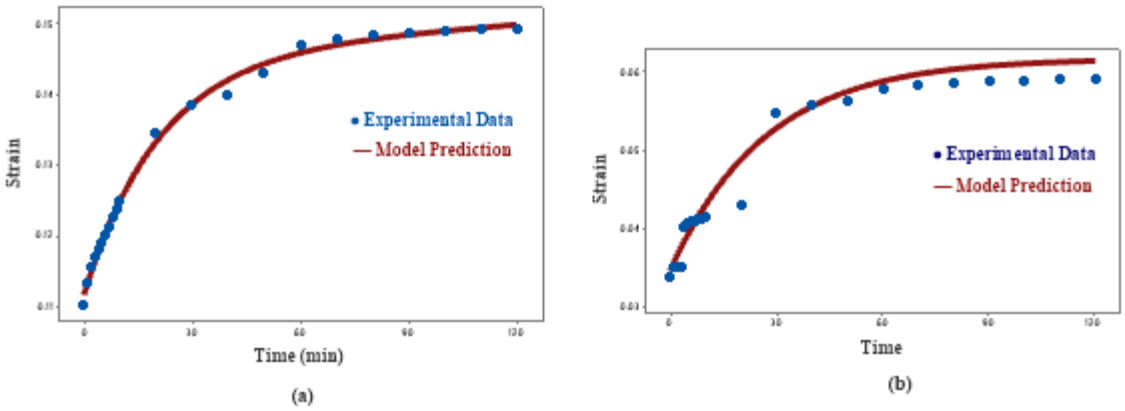

Figure 5. Comparison of experimental data and Burgers model predictions: (a) 2-layer seamless, (b) 6-layer seamed.

3.2. ANALYSIS OF VISCOELASTIC PARAMETERS

Investigation of the viscoelastic parameters extracted for seamed specimens with varying numbers of layers (2, 6, 12, and 24), presented in Table 2, the behavior of the instantaneous elastic modulus (E_M)—which represents the resistance of the seam structure to instantaneous deformation—exhibits the most distinct non-linear trend. As the number of layers increased from 2 to 6, the initial stiffness expectedly increased more than threefold, rising from 15.51 ± 0.17 to 47.88 ± 0.73 MPa. This enhancement is attributed to the increased seam thickness and structural compactness. In the 12-layer specimen, a remarkable, approximately tenfold surge in seam stiffness occurred compared to the 6-layer specimen, reaching a peak value of 459.10 ± 9.33 MPa. This extraordinary increase indicates the formation of a highly efficient and integrated seam structure, wherein the interaction between the layers and the sewing thread reached its optimal state of structural cohesiveness. However, this upward trend did not persist. With a further increase to 24 layers, the initial stiffness sharply declined, reverting to 48.15 ± 0.67 MPa, a value comparable to that of the 6-layer specimen. This drastic drop in performance suggests that beyond an optimal point, increasing thickness becomes detrimental, leading to reduced mechanical efficiency of the entire structure due to phenomena such as internal layer buckling (micro-buckling) or non-uniform stress distribution among the multiple layers. This finding demonstrates the existence of an optimal number of layers to achieve maximum stiffness within the seam structure.

Textile Science & Research Journal
ISSN: 3059-846X, Volume – 2, Issue – 1, 2026
DOI: https://doi.org/10.63456/tsrj-2-1-39

Table 2. Viscoelastic parameters obtained from the Burgers model for the seamed specimens.

Sample	σ_0 (MPa)	E_M (MPa)	E_V (MPa)	η_V (Mpa.s)	η_M (Mpa.s)
2-layer seamed	1.426	15.51 ± 0.17	76.48 ± 6.60	355.17 ± 36.25	17382.17 ± 1901
6-layer seamed	1.657	47.88 ± 0.73	62.55 ± 1.27	1554.50 ± 69.93	∞
12-layer seamed	1.597	459.10 ± 9.33	230.43 ± 3.32	557.75 ± 65.96	∞
24-layer seamed	0.939	48.15 ± 0.67	63.77 ± 6.30	699.92 ± 52.75	∞

The behavior of the retardation parameters, which characterize the time-dependent dynamics of the creep process, further complicates and corroborates the observed non-linear trend. The Kelvin-Voigt viscosity (η_V)—representing the resistance to delayed viscoelastic deformation—exhibits a significant increase from 355.17 ± 36.25 MPa.s in the 2-layer seamed specimen to a peak of 1554.50 ± 69.93 MPa.s in the 6-layer configuration. This drastic rise indicates a structure with high internal friction, which significantly delays the internal rearrangement process. Consequently, the derived retardation time ($\tau = \eta_V/E_V$) reaches its most sluggish state in the 6-layer specimen.

Subsequently, in the 12-layer specimen, η_V drops to 557.75 ± 65.96 MPa.s. Combined with the exceptionally high delayed elastic modulus (E_V) of 230.43 ± 3.32 MPa observed in this structure (Table 2), the system achieves its fastest stabilization dynamics, with τ decreasing to approximately 2.42 min. This signifies a shift in energy dissipation mechanisms, where the 12-layer seam functions as a dense, interlocked, and efficient unit. In contrast, the 24-layer structure shows a resurgence in delayed resistance (η_V = 699.92 ± 52.75 MPa.s), indicating that excessive thickness again hinders rapid stabilization. These results demonstrate that among the investigated discrete layer counts, the 12-layer seamed configuration represents a peak performance point, exhibiting a superior balance of both structural stiffness and dynamic stabilization speed. The engineering significance of these findings is particularly relevant for high-performance technical insulation systems where long-term dimensional stability is a prerequisite for functional reliability. In such multi-layer assemblies, the recorded creep strain levels can lead to structural sagging or localized misalignment at the seam zones. These structural changes can facilitate unexpected heat leakage (thermal bridging), which reduces the overall thermal efficiency of the system. Therefore, the enhanced stability observed in the 12-layer configuration is required for maintaining the structural integrity of complex insulation blankets under prolonged stress.

To establish a baseline for evaluating the net effect of the seam, the viscoelastic properties of seamless specimens with varying numbers of layers (2, 6, 12, and 24) were investigated as a control group. Analyzing the behavior of these specimens provides deep insight into the intrinsic properties of the multi-layer textile structure. The quantitative results derived from the Burgers model fitting for these specimens are summarized in Table 3.

Table 3. Viscoelastic parameters of the seamless specimens.

Sample	σ_0 (MPa)	E_M (MPa)	E_V (MPa)	η_V (Mpa.s)	η_M (Mpa.s)
2-layer seamless	3.765	34.02 ± 0.05	113.85 ± 8.46	2194.45 ± 193.29	119968 ± 63249
6-layer seamless	2.168	49.48 ± 1.02	202.07 ± 17.51	165.95 ± 28.51	40979 ± 5992.73
12-layer seamless	2.039	-	-	-	-
24-layer seamless	1.304	50.27 ± 0.91	352.23 ± 25.28	224.07 ± 61.13	159412.9 ± 35594

The results presented in Table 3 reveal a general upward trend for both instantaneous (E_M) and delayed (E_V) moduli with increasing layer count in the seamless specimens (excluding the 12-layer configuration). The instantaneous modulus increased from 34.02 ± 0.05 Mpa (2-layer) to 50.27 ± 0.91 MPa (24-layer). This increase is attributed to the increased thickness and cross-sectional area, yielding greater resistance to instantaneous deformation. This trend is even more pronounced for the delayed elastic modulus, which rose from 113.85 ± 8.46 to 352.23 ± 25.28 MPa. This indicates that thicker structures exhibit significantly higher resistance to time-dependent deformation (creep) due to enhanced surface interactions and internal friction between layers. It is important to note that the 12-layer seamless specimen is excluded from this trend analysis due to its inherent structural instability, which prevented mathematical convergence during the modeling process.

In seamless specimens, a significant reduction in the retardation viscosity (η_V) occurred as the layer count increased. As detailed in Table 2, η_V decreased from 2194.45 ± 193.29 MPa.s (2-layer) to 224.07 ± 61.13 MPa.s (24-layer). This decline,

Textile Science & Research Journal
ISSN: 3059-846X, Volume – 2, Issue – 1, 2026
DOI: https://doi.org/10.63456/tsrj-2-1-39

combined with the increasing delayed elastic modulus (E_V), led to the derived retardation time ($\tau = \eta_V/E_V$) plummeting from 19.27 min to 0.64 min. This suggests that thicker seamless assemblies reach mechanical stabilization significantly faster, likely due to increased surface interactions and interlayer friction in high-ply configurations. Unlike seamed structures, where sewing threads provide external pressure and mechanical consolidation, the stabilization in these control specimens is driven primarily by the internal surface contact area of the stacked layers.

Regarding the 12-layer seamless specimen, the Burgers model failed to reach mathematical convergence, manifesting irregular creep rate oscillations. This suggests an inherent structural instability at this specific layer count. In the absence of sewing threads to integrate the assembly, the 12-layer structure appears unable to sustain a unified mechanical response, behaving as a transitional state between loosely coupled thin structures and self-stabilized thick structures. This anomaly highlights the critical role of the stitched seam, which effectively stabilizes this inherently unstable configuration, as demonstrated by the successful convergence and superior stiffness observed in the 12-layer seamed specimens.

3.3. COMPARATIVE ASSESSMENT OF SEAM IMPACT

To elucidate the impact of the presence of the seam, a pairwise comparative analysis was conducted between seamed and seamless specimens at each layer count. This analysis reveals that the seam functions not merely as a passive connector but as an active element whose interaction with the structure yields diametrically opposed outcomes depending on the layer count and cross-sectional thickness.

As illustrated in Fig. 6, a 54.4% reduction in the initial stiffness of the 2-layer seamed specimen compared to its seamless counterpart indicates that in a structure with low cross-sectional thickness, the physical damage induced by the sewing process (specifically needle penetration and localized rupture of the fabric and polymeric film substrates) compromises the structural integrity of the fabric in the seam zone, transforming it into a stress concentration zone that leads to higher instantaneous deformation. Conversely, a significant reduction in the independent Kelvin-Voigt viscosity (η_V) for the 2-layer seamed specimen shown in Fig. 7 suggests that this damaged structure provides new pathways for slippage and faster layer rearrangement. Consequently, the system reaches its viscoelastic equilibrium more rapidly. Thus, in the lowest layer count examined, the seam weakens mechanical properties but accelerates dynamic response.

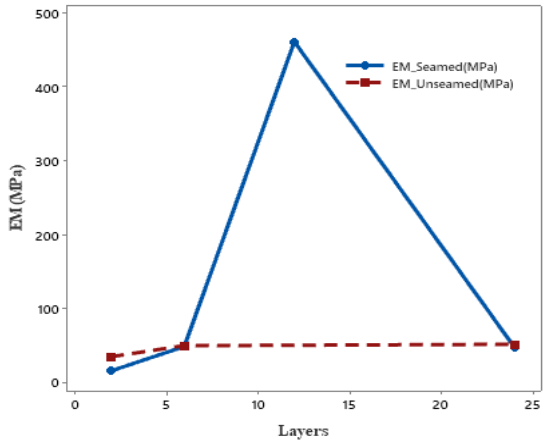

Figure 6. Comparison of the instantaneous elastic modulus of seamed and seamless specimens with different numbers of layers.

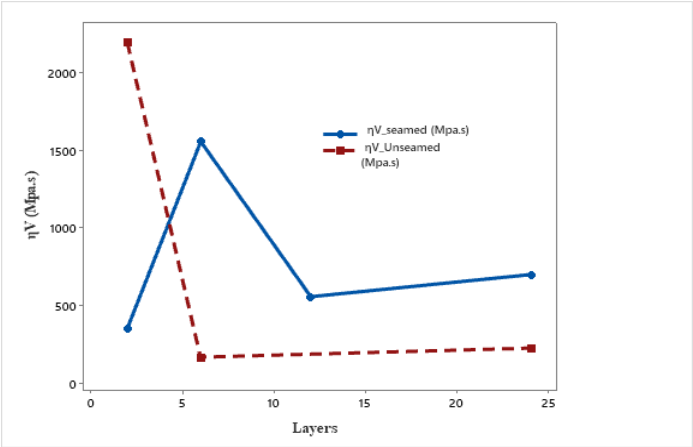

Figure 7. Comparison of the Kelvin-Voigt viscosity (η_V) for seamed and seamless specimens with different numbers of layers

Textile Science & Research Journal
ISSN: 3059-846X, Volume – 2, Issue – 1, 2026
DOI: https://doi.org/10.63456/tsrj-2-1-39

Fig. 6 and Fig. 7 demonstrate that as the layer count increases to 6, the seam exerts a divergent influence. The initial stiffness (E_M) remains virtually unchanged, indicating that at this thickness, needle damage is compensated by layer compaction and the presence of the sewing thread. However, the Kelvin-Voigt viscosity (η_V) increased significantly. The 6-layer seamless fabric is a compact structure that reaches equilibrium in less than a minute. Seam formation induces friction and complex interactions between layers and thread, transforming it into a sluggish structure with high energy dissipation, significantly delaying the equilibrium process. Therefore, the presence of the seam in the 6-layer structure does not alter initial stiffness but slows down system dynamics by introducing new energy dissipation mechanisms.

As discussed, the 12-layer seamless structure was inherently unstable. In contrast, seam formation transformed this unstable assembly into the specimen with the highest mechanical performance in this study (an approximately tenfold surge in (E_M) compared to the 6-layer specimen and the fastest dynamic response). The sewing threads likely prevented internal buckling and slippage, creating a structurally cohesive unit. This synergistic effect underscores the critical importance of the seam-fabric interaction in this optimal structure. This proposed mechanism of structural cohesion and interlocking, where the seam acts as a vertical reinforcement to prevent internal buckling and slippage, is conceptually illustrated in Fig. 8.

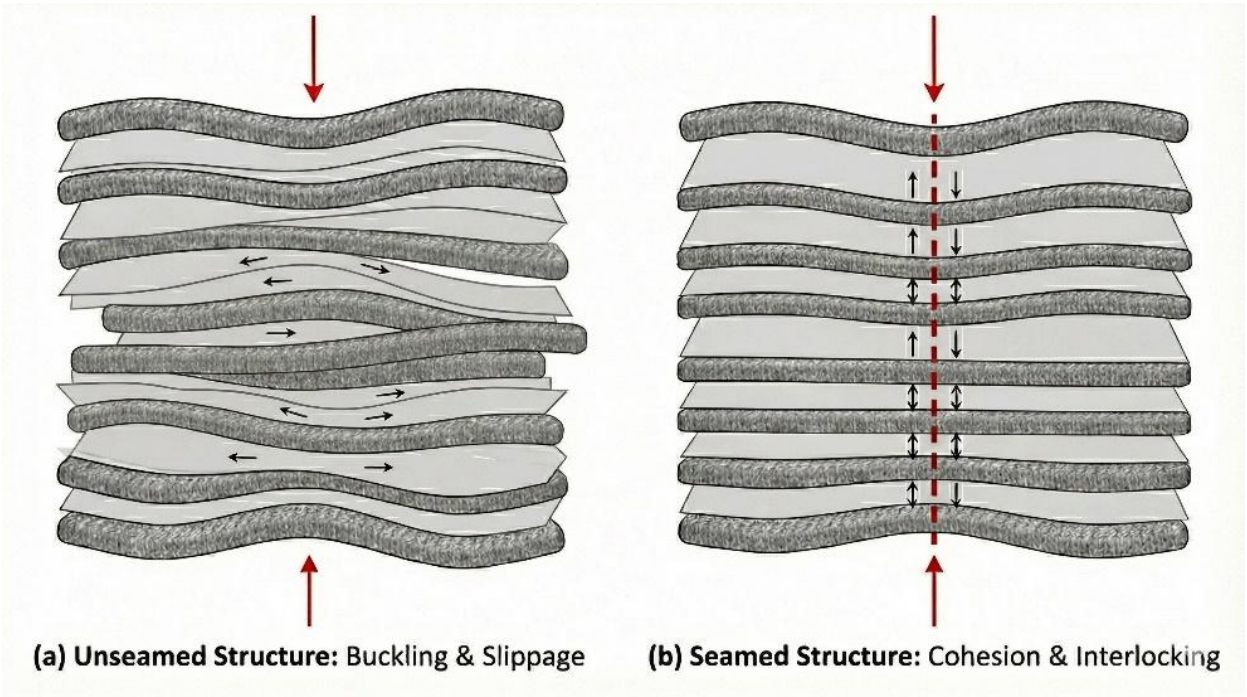

Figure 8. Schematic illustration of the 12-layer structure showing (a) buckling and slippage in the seamless configuration versus (b) structural cohesion and interlocking in the seamed assembly.

The behavior observed in the 24-layer structure corroborates the pattern seen in the 6-layer structure. As shown in Fig. 6 and Fig.7, the initial stiffness shows little difference between seamed and seamless 24-layer samples, yet the viscosity (η_V) increases with the presence of the seam. These results confirm that in very thick structures, the dominant mechanism of the seam's impact is the generation of internal friction and the retardation of system dynamics. The performance drop of the 24-layer seamed specimen compared to the optimal 12-layer one further indicates that the reinforcing effect observed at 12 layers diminishes with excessive thickness and compaction in the seam section. Thus, in highly thick structures, the seam acts as a disruptive element that significantly reduces the dynamic efficiency of the system.

3.4. MODEL VALIDATION VIA SEAM CREEP RATE DYNAMICS

To provide physical, model-independent verification of the complex dynamics inferred from the viscoelastic parameters of the Burgers model, creep rate analysis was employed as a complementary phenomenological approach. This analysis reveals the instantaneous speed of material deformation and offers deep insight into how the structure approaches viscoelastic equilibrium.

Direct comparison of creep rate plots for seamed and seamless specimens visually demonstrates the dual, thickness-dependent impact of the seam. As observed in Fig. 9, the 2-layer seamless specimen shows a slow, gradual decline in creep rate. In contrast, the seamed specimen experiences a rapid, instantaneous drop. This comparison clearly demonstrates that the seam has accelerated the system dynamics.

Textile Science & Research Journal
ISSN: 3059-846X, Volume – 2, Issue – 1, 2026
DOI: https://doi.org/10.63456/tsrj-2-1-39

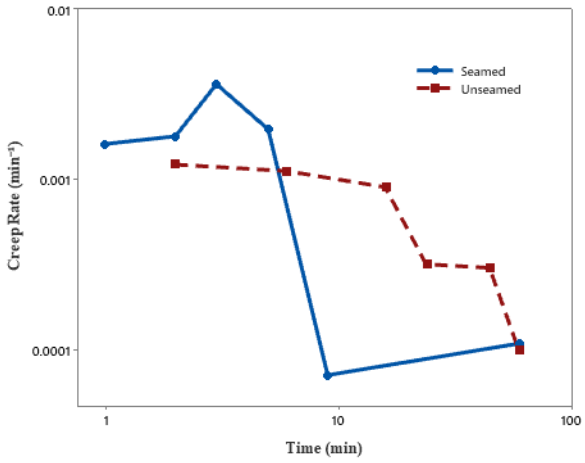

Figure 9. Comparison of creep rate versus time for 2-layer seamed and seamless specimens on a log-log scale.

Looking at Fig. 10, this trend is completely reversed for the 6-layer structure. The seamless specimen exhibits very fast dynamics, where the creep rate drops to low values almost immediately. Conversely, the seamed specimen shows a very slow, prolonged rate reduction process. This stark contrast provides physical proof that as the layer count increases, the seam significantly retards system dynamics by inducing internal friction.

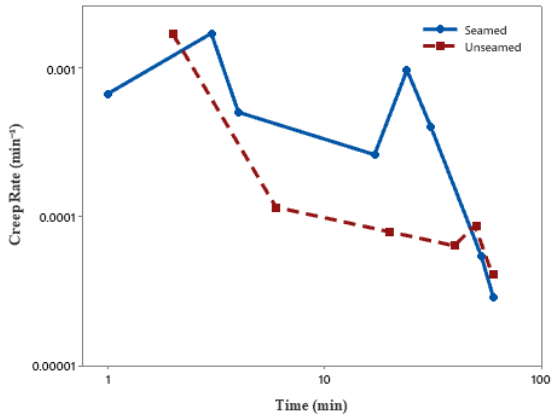

Figure 10. Comparison of creep rate versus time for 6-layer seamed and seamless specimens on a log-log scale.

As seen in Fig. 11, the creep rate plot for the 12-layer seamless specimen displays a highly irregular, fluctuating behavior. Lacking any distinct decaying trend, this plot serves as the best visual evidence of the inherent instability of this structure, explaining why the mathematical Burgers model failed to converge. In contrast, the 12-layer seamed specimen exhibits the fastest and most efficient decaying dynamic among all seamed samples. The rapid drop in creep rate within the very first minutes visually confirms the dynamic optimality of this structure.

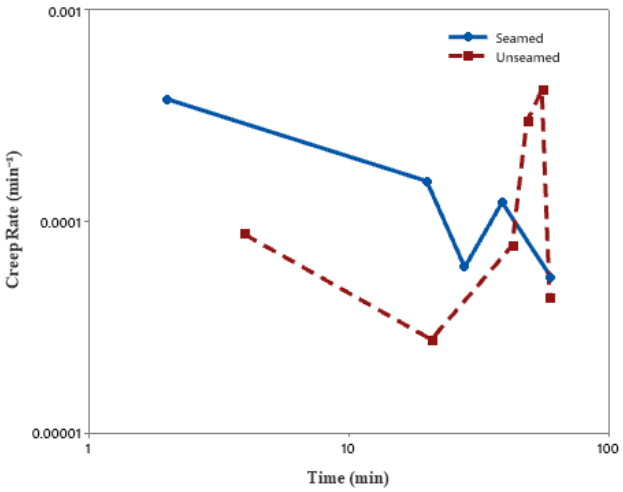

Figure. 11. Comparison of creep rate versus time for 12-layer seamed and seamless specimens on a log-log scale.

Textile Science & Research Journal
ISSN: 3059-846X, Volume – 2, Issue – 1, 2026
DOI: https://doi.org/10.63456/tsrj-2-1-39

The behavior observed in the thickest specimen (24-layer) reinforces the pattern seen in the 6-layer structure. As clearly seen in Fig. 12, the dynamics of the seamed and seamless structures are diametrically opposed. The seamless specimen shows a rapid, instantaneous drop in creep rate, indicating a compact, efficient structure with a near-instantaneous dynamic response. This aligns perfectly with the very short derived retardation time ($\tau = 0.64$ min) calculated from the Burgers model. Conversely, the seamed specimen displays a completely different behavior; the creep rate remains high and nearly constant for about 10 minutes before declining. This initial lag phase provides visual proof of the longer calculated response time ($\tau = 10.98$ min) and indicates that the presence of the seam has delayed the internal rearrangement process.

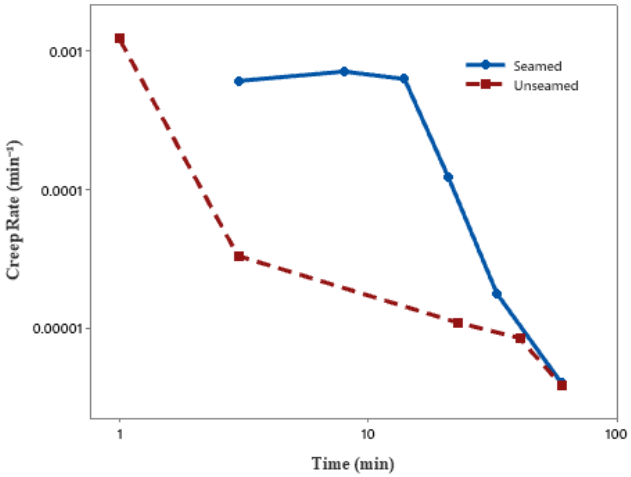

Figure. 12. Comparison of creep rate versus time for 24-layer seamed and seamless specimens on a log-log scale.

Finally, the simultaneous observation of the four creep rate plots for seamed specimens in Fig. 13 directly validates the parametric findings extracted from the Burgers model. The evident differences in creep rate reduction dynamics-including the very slow trends versus the rapid drops observed in this plot-correspond perfectly with the non-uniform trends and contrasting values of the stabilization dynamics obtained from the Burgers viscoelastic model. This convergence of results derived from two independent analytical approaches (parametric modeling and phenomenological analysis) lends significant validity to the overall findings, strongly supporting the central hypothesis of a non-linear optimal behavior.

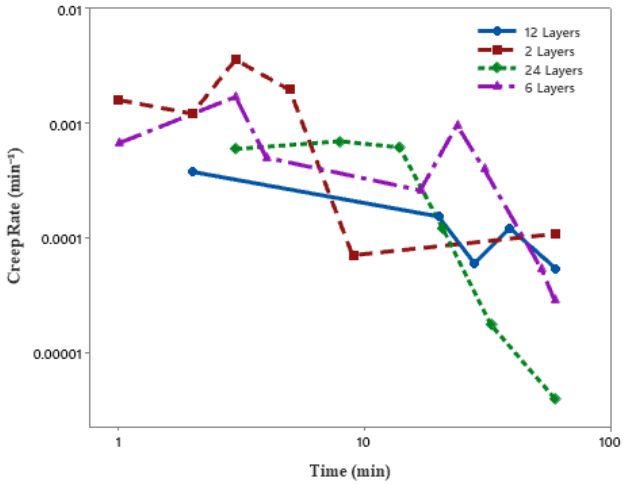

Figure. 13. General comparison of creep rate reduction dynamics in seamed specimens with different numbers of layers.

4. CONCLUSIONS

In this study, the viscoelastic creep behavior of the seam zone in multi-layer hybrid textile structures was comprehensively investigated using a dual-analysis methodology comprising Burgers parametric modeling and phenomenological creep rate analysis. The key findings of this research are:

- Non-linear Relationship and Performance Peak: It was demonstrated that the relationship between the number of layers and the seam's viscoelastic properties is non-linear. Mechanical performance—both in terms of instantaneous and delayed stiffness—reaches a distinct peak in the 12-layer configuration, followed by a sharp decline in performance with further layer increase due to structural instabilities. This indicates that within the investigated

discrete range, the 12-layer configuration represents a peak performance point, characterized by a superior balance between structural stiffness and dynamic stabilization speed.

- Dual and Thickness-Dependent Role of the Seam: It was concluded that the seam's impact on fabric properties is contingent upon cross-sectional thickness. In thin structures (2 layers), the seam acts as a structural defect, significantly reducing instantaneous stiffness (weakening effect). Conversely, in thick structures (24 layers), the seam fundamentally alters system dynamics by introducing significant internal friction and viscous resistance (η_V), which leads to a longer derived response time τ (retarding effect).
- Seam Stabilizing Role in the Peak-Performance Configuration: The most significant finding was the seam's role as a vital stabilizing element in the 12-layer configuration. While the 12-layer seamless specimen exhibited inherent instability and irregular creep behavior that prevented mathematical convergence, seam formation transformed this unstable structure into a structurally cohesive, efficient system with the highest stiffness (E_M) and the fastest calculated dynamic response (lowest τ). This indicates that at this observed peak (12 layers), the seam functions beyond a mere connector, acting as a structural reinforcement and stabilizing element.

This research highlights the necessity of understanding the complex, non-linear interaction between the seam structure and the number of layers for the optimal design of multi-layer insulating structures. The results provide a rigorous engineering framework for designing multi-layer structures with superior mechanical performance and time-dependent dimensional stability.

Future Research: While the 12-layer configuration exhibited the peak performance within the discrete dataset investigated, the complex non-linear trends identified here suggest a fertile ground for advanced computational modeling. Future research could focus on utilizing optimization algorithms—such as Genetic Algorithms (GA) or Artificial Neural Networks (ANN)—to explore the multi-dimensional parameter space more granularly. This would enable the identification of the precise global optimal layer count and seam density, further refining the engineering design of high-performance technical insulation textiles

REFERENCES:

[1] M. Shamsuyeva, J. Winkelmann, and H.-J. Endres, "Manufacture of hybrid natural/synthetic fiber woven textiles for use in technical biocomposites with maximum biobased content," *Journal of Composites Science*, vol. 3, no. 2, p. 43, 2019.
[2] T. Miyakita, R. Hatakenaka, H. Sugita, M. Saitoh, and T. Hirai, "Development of a new multi-layer insulation blanket with non-interlayer-contact spacer for space cryogenic mission," *Cryogenics*, vol. 64, pp. 112–120, 2014.
[3] Davies and J. Williams, "The use of spacer fabrics for absorbent medical applications," *Journal of Fiber and Bioengineering and Informatics*, vol. 1, no. 4, pp. 321–330, 2009.
[4] N. Gokarneshan and K. Velumani, "Some significant advances in spacer fabric technology for newer areas of applications," *J Textil Sci Eng*, vol. 8, pp. 1–5, 2018.
[5] H. Mesforoush, M. Pakmanesh, H. Esfandiary, S. Asghari, and E. Baniasadi, "Experimental and numerical analyses of thermal performance of a thin-film multi-layer insulation for satellite application," *Cryogenics*, vol. 102, pp. 77–84, 2019.
[6] B. Rajput, M. Kakde, S. Gulhane, S. Mohite, and P. Raichurkar, "Effect of sewing parameters on seam strength and seam efficiency," *Trends in Textile Engineering and Fashion Technology*, vol. 4, no. 1, pp. 4–5, 2018.
[7] E. Z. Yıldız and O. Pamuk, "The parameters affecting seam quality: a comprehensive review," *Research Journal of Textile and Apparel*, vol. 25, no. 4, pp. 309–329, 2021.
[8] H.-J. Chun, H.-W. Kim, and J.-H. Byun, "Effects of through-the-thickness stitches on the elastic behavior of multi-axial warp knit fabric composites," *Composite Structures*, vol. 74, no. 4, pp. 484–494, 2006.
[9] Y. Admassu, A. Edae, G. Getahun, S. Senthil Kumar, K. Saravanan, and S. Sakthivel, "Experimental analysis on the effect of fabric structures and seam performance characteristics of weft knitted cotton apparels," *Journal of Engineered Fibers and Fabrics*, vol. 17, p. 15589250221113479, 2022.
[10] Gurarda, "Seam performance of garments," *Textile Manufacturing Processes*, vol. 5, p. 17, 2019.
[11] T. Ohmori, M. Nakajima, A. Yamamoto, and K. Takahashi, "Lightweight multilayer insulation to reduce the self-compression of insulation films," in *AIP Conference Proceedings*, vol. 613, no. 1, American Institute of Physics, pp. 1565–1572, 2002.
[12] J. G. Telles Ribeiro and A. Cunha Jr, "Advanced creep modelling for polymers: a variable-order fractional calculus approach," *Proceedings of the Royal Society A*, vol. 481, no. 2322, p. 20240861, 2025.
[13] Y. Gao, B. Zhao, D. Yin, and L. Yuan, "A general fractional model of creep response for polymer materials: Simulation and model comparison," *Journal of Applied Polymer Science*, vol. 139, no. 5, p. 51577, 2022.
[14] J. G. T. Ribeiro and A. Cunha Jr, "Advanced creep modelling for polymers: A variable-order fractional calculus approach," *arXiv preprint arXiv:2510.11765*, 2025.
[15] G. Spathis and E. Kontou, "Creep failure time prediction of polymers and polymer composites," *Composites Science and Technology*, vol. 72, no. 9, pp. 959–964, 2012.
[16] Gürarda and B. Meriç, "Slippage and grinning behaviour of lockstitch seams in elastic fabrics under cyclic loading conditions," *Textile and Apparel*, vol. 20, no. 1, pp. 65–69, 2010.

[17] K. Kabish, "Effects of dynamic loading of sewing process and viscoelastic property of threads on seam puckering," *Journal of Textile and Apparel, Technology and Management*, vol. 8, no. 4, 2014.
[18] R. Zadekhast and A. Asayesh, "Evaluation of the tensile creep behavior of various warp knitted fabric structures using viscoelastic models," *Fibers and Polymers*, vol. 24, no. 7, pp. 2479–2489, 2023.
[19] Mukhopadhyay and V. Midha, "The quality and performance of sewn seams," in *Joining Textiles*, Elsevier, pp. 175–207, 2013.
[20] M. A. Seif, "Investigating the seam slippage of satin fabrics," *International Journal of Textile and Fashion Technology*, vol. 4, no. 5, pp. 1–10, 2014.
[21] X. Gao, H. Chen, and S. Sun, "Analysis of the creep properties of nonwoven fabric with mechanical models," *Fibres & Textiles in Eastern Europe*, no. 1 (109), pp. 72–76, 2015.
[22] N. Mandlekar, B. Rana, P. Maurya, B. S. Butola, and M. Joshi, "Long-term prediction of creep and stress-relaxation behaviour in synthetic fabrics using the time–temperature superposition principle," *Fibers and Polymers*, vol. 24, no. 6, pp. 2195–2207, 2023.
[23] E. Secretariat, *Thermal Design Handbook–Part 7: Insulations*, 2011.